Sigma J Eng & Nat Sci 38 (2), 2020, 603-612

Sigma Journal of Engineering and Natural Sciences
Sigma Mühendislik ve Fen Bilimleri Dergisi

Research Article

CFD ANALYSIS OF MINI VENTURI-TYPE AIR FLOWMETERS FOR LAB-SCALE APPLICATIONS

Selami DEMİR*[1]

[1]*Yildiz Technical University, Environmental Eng. Department, İSTANBUL;* ORCID: 0000-0002-8672-9817

Received: 23.01.2020 Revised: 09.02.2020 Accepted: 11.02.2020

ABSTRACT

Being one of the cheapest devices for air flow measurement within a wide range of flowrates, Venturi-type air flowmeters (VTAFs) can also be used for measuring very small air flowrates, usually less than 50 to 100 liters per minute, which is usually encountered in lab-scale applications. This study presents a model-based evaluation of VTAFs for lab-scale applications. The pressure and velocity fields in mini VTAFs were calculated by computational fluid dynamics (CFD) model using Ansys Fluent™. Results showed that sensitive and accurate measurements of volumetric flowrate can be achieved using mini VTAFs. A diameter ratio of 0.6 for the venturi throat provides a minimum detection limit of 2.46 LPM while an overall pressure drop of around 115 Pa at an air flowrate of 50 LPM at 20°C.
Keywords: Air flow, mesasurement, lab-scale applications, venturi flowmeters.

1. INTRODUCTION

Influent air or water flowrate is of vital importance for a wide range of treatment processes from water and wastewater treatment to air pollution control systems. There are a great number of flow measuring devices, which can be classified as ultrasonic, differential pressure, positive displacement, and mass flowmeters [1]. For especially in laboratory-scale applications where relatively small flows of air or water are encountered, ultrasonic or mass flowmeters are usually preferred if accurate and precise measurement of flowrate is required. However, mass flowmeters come with relatively high-cost which leads to increased cost of research work in almost all cases. Zhang et al [2] reported that flowmeters of differential pressure type can be preferred over other types of flow measuring devices considering the fact that they have no risks of radiation and no limitation pertaining to fluid conductance, etc. Besides, their cost is considerably low compared to other devices.

Air flowmeters of differential pressure type can be of various designs, including orifice plate flowmeters, details of the design of which can be found in the international standard ISO 5167-2:2003, and pipe flowmeters, both of which can be employed to accurately measure air flowrate. For instance, Demir [3] and Demir et al [4] reported successful use of an orifice plate air flowmeter for a lab-scale cyclone separator system, while Demir et al [5] discussed the problem of air flow measurement in a pipe. Another type of differential pressure air flowmeters is the

* Corresponding Author: e-mail: seldemir@yildiz.edu.tr, tel: (212) 383 53 72

venturi-type flowmeters, details of the design of which are given in the international standard (ISO 5167-4:2003). Venturi flowmet ers can be very accurate devices of air flow measurement without the risks mentioned above. A great number of research has been dedicated to differential pressure type flowmeters including venturi tubes, some of which can be found in [1, 6-16].

To the author's experience, lab-scale water and wastewater treatment systems are designed for up to a few liters per hour of influent, while usually less than 50 to 100 liters per minute of air flowrates are used in most lab-scale air purification systems. In lab-scale systems, one needs precise measurements of flowrate as low as that can be measured with devices designed to produce a signal proportional to these low ranges. Properly sized venturi-type flowmeters can meet these needs.

A venturi-type flowmeter is a device which relies on the measured difference of static pressures at specific sections within. It basically creates sensible change of static pressure by reduced cross-section over the course of the pipe. The pressure drop (called overreading) is then proportional to the air flowrate. The overreading is usually measured between the upstream (also called divergent) section and throat section of the venturi. The international standard for the design of venturi flowmeters (ISO 5167-4: 2003) describes the main criteria for an accurate flow measuring device. Once the mentioned criteria are met, one can use the following formula to calculate the mass flowrate of the fluid using the overreading and several fluid properties:

$$q_m = \frac{1}{4} c\varepsilon\pi d^2 \sqrt{\frac{2\rho_1 \Delta p}{1-B^4}} \quad (1)$$

where c is the discharge coefficient of the venturi, ε is the expansibility factor, d is the throat section diameter, ρ_1 is the density of the fluid in the upstream section, B is the ratio of the diameter of the upstream section to that of throat section, and q_m is the mass flowrate of the fluid, which can then be used to express volumetric flowrate as follows:

$$q_v = \frac{q_m}{\rho} \quad (2)$$

where q_v is the volumetric flowrate and ρ is the density of the fluid at the temperature and pressure for which the volume is stated.

Although the international standard (ISO 5167-4: 2003) does not cover venturi flowmeters of pipe diameters less than 50 mm, it is the author's opinion that the success of a venturi-type flowmeter depends on the degree to which a sensible signal (pressure drop) is produced, which is accurately proportional to the flowrate of the fluid. Now that great advancements have been achieved in the field of electronics and sensing devices, it is possible to employ differential pressure transmitters that is capable of sensing very small pressure differences. Besides, production of venturis is easier with the help of 3D printing technologies. Considering the above-mentioned advancements in sensing and production technology, it is the author's opinion that a very sensitive and accurate mini venturi-type air flowmeter can be manufactured to use in most lab-scale applications.

The aim of this study is to evaluate the performances of mini venturi-type air flowmeters (VTAFs) based on model results. This is accomplished by running computational fluid dynamics (CFD) model using ANSYS Fluent™. For this purpose, pressure and velocity fields on several VTAFs for air flowrates up to 50 liters per minute at 20°C were calculated. A total of nine VTAFs with three different diameter ratios and three different divergent angles were evaluated based on their response curves and overall pressure drops.

2. MATERIALS AND ME THODS

2.1. Flowmeter Design

The mini venturi-type flowmeters for dry air flowrates up to 50 LPM were designed for modeling study. The flowmeters were composed of three main body parts: the convergent section, the throat section, and the divergent section. The diameter of the convergent and the divergent sections (*D*) were 10 mm. The convergent angle (A_c) was 21°. All converging and diverging sections were rounded with radii of curvature equal to 10 mm. Nine venturi tubes were created based on the throat diameter (*d*) and the divergent angle (A_d). For this purpose, three throat diameters of 5, 6, and 7 mm were used, corresponding to diameter ratios (*B*) of 0.5, 0.6, and 0.7. Three divergent angles were used as 7°, 11°, and 15°. The total length of the flowmeters was 100 mm with the center of the throat located at 50 mm from the entrance of the convergent section. Schematics of the venturi flowmeters are shown in Fig. 1 and the dimensions are shown in Table 1.

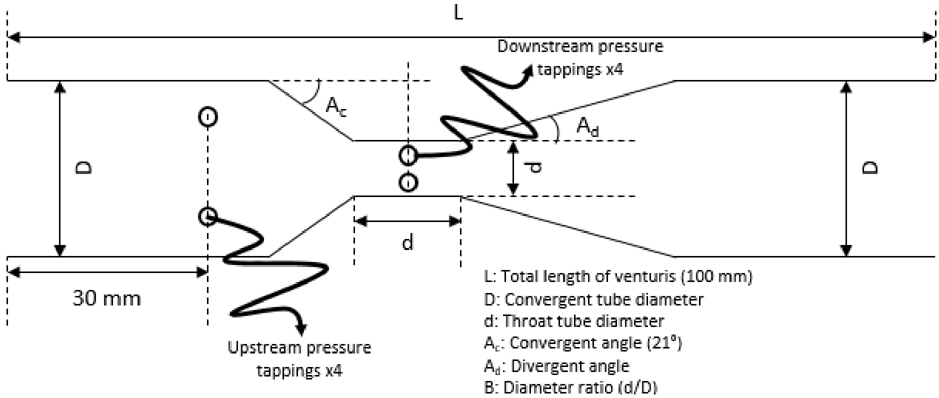

Figure 1. Schematics of venturi-type air flowmeters

Table 1. Dimensions of venturi-type air flowmeters

Venturi Code	Throat tube diameter (d, mm)	Diameter ratio (B)	Divergent angle (A_d)
B5A07	5	0.5	7°
B5A11	5	0.5	11°
B5A15	5	0.5	15°
B6A07	6	0.6	7°
B6A11	6	0.6	11°
B6A15	6	0.6	15°
B7A07	7	0.7	7°
B7A11	7	0.7	11°
B7A15	7	0.7	15°

For all flowmeters, upstream pressure tappings were located at 30 mm from the entrance of the convergent section and the downstream pressure tappings were located at the center of the throat. Four tappings were used with 90° spacing for both upstream and downstream pressure probing to obtain a reliable average of pressure drop within the venturi flowmeters.

2.2. Fluent Options

ANSYS Fluent™ 2019 R1 coupled with ANSYS SpaceClaim, ANSYS Mesh Modeler and ANSYS CFD-Post was used for modeling. The solid models were created using ANSYS SpaceClaim, and were meshed using ANSYS Mesh Modeler. For meshing, the size of the tetrahedrons was selected between $0.5*10^{-4}$ and $0.7*10^{-4}$ m and inflation layers were created around the outer walls. A total of 135,834 to 285,314 cells were created for all of nine flowmeters.

The inlet of the flowmeters was set as velocity inlet with defined values of flow velocities. The outlet was set as pressure outlet with zero gage pressure, while the roughness of the walls was set as 0.1 mm. A maximum number of iterations of 1,000 was used. The viscous model was realizable k-ε with standard wall functions, which is one of the most accurate models for most linear flow systems. The pressure-velocity coupling scheme was selected as PISO with the options shown in Table 2.

Table 2. Spatial discretization options for steady-state simulation of flowmeters

Discretization type	Option
Gradient	Least squares cell based
Pressure	PRESTO!
Momentum	QUICK
Turbulent kinetic energy	Second order upwind
Turbulent dissipation rate	Second order upwind

3. RESULTS AND DISCUSSIONS

3.1. Measurement Limits

The first step of the simulation was the determination of the level of meshing. For this purpose, a mesh-dependency test was performed, in which the solid models for each venturi flowmeter were meshed with three different levels of meshing, namely coarse, moderate, and fine meshing. Then, steady-state simulations were run with each level of meshing. For all simulations, the inlet velocity was set as 10 m/s, which corresponds to 47.12 LPM of dry air flow at 20°C. All of the solutions were converged around 300^{th} to 450^{th} iteration. The results are summarized in Table 3, where the pressure drops were calculated as the difference of area-weighted static pressures between the inlet and the outlet of the flowmeters. Percent discrepancies in Table 3 were calculated using the arithmetic average of the calculated pressure drops over the flowmeters. All of the calculated discrepancies were very small (under 1%). Thus, the coarser meshing was used for all flowmeters to save computational power and time.

One can expect that the pressure drop across the flowmeter is a measure of the cost of measurement in that a good flowmeter is the one which results in very small overall pressure drop while sustaining good accuracy and sensitivity. Results in Table 3 can also be interpreted as the cost of measurement in terms of pressure drop across the flowmeter. As expected, the overall pressure drop was a function of the diameter ratio of the flowmeter: The higher the diameter ratio is, the lower the overall pressure drop is. Therefore, the flowmeters with the diameter ratio 0.7 (B7A07, B7A11, and B7A15) caused the lowest overall pressure drops. The results, on the other hand, showed that the divergent angle is also effective on the overall pressure drop. It is clear that the flowmeter with the lowest divergent angle (B7A07) offers the lowest pressure drop, thus the lowest cost of measurement.

Table 3. Results of mesh-dependency check for simulations

Flowmeter	**Parameter**	**Coarse meshing**	**Moderate meshing**	**Fine meshing**
B5A07	Mesh	135,834	198,902	268,808
	Pressure drop (Pa)	257.6	254.4	253.5
	Percent discrepancy	0.94%	0.31%	0.67%
B5A11	Mesh	140,700	204,770	274,060
	Pressure drop (Pa)	283.3	283.4	281.0
	Percent discrepancy	0.25%	0.28%	0.57%
B5A15	Mesh	141,281	207,346	277,319
	Pressure drop (Pa)	304.3	306.7	304.8
	Percent discrepancy	0.33%	0.46%	0.16%
B6A07	Mesh	142,837	204,571	276,621
	Pressure drop (Pa)	115.4	114.1	115.0
	Percent discrepancy	0.52%	0.61%	0.17%
B6A11	Mesh	144,846	207,246	280,362
	Pressure drop (Pa)	122.2	121.5	122.0
	Percent discrepancy	0.25%	0.33%	0.08%
B6A15	Mesh	145,581	209,708	282,168
	Pressure drop (Pa)	128.9	127.4	129.0
	Percent discrepancy	0.39%	0.78%	0.47%
B7A07	Mesh	145,936	209,158	284,371
	Pressure drop (Pa)	63.7	63.6	63.5
	Percent discrepancy	0.21%	0.05%	0.26%
B7A11	Mesh	147,506	211,878	284,234
	Pressure drop (Pa)	64.0	64.6	65.0
	Percent discrepancy	0.83%	0.10%	0.72%
B7A15	Mesh	147,690	214,103	285,314
	Pressure drop (Pa)	67.1	67.7	67.9
	Percent discrepancy	0.74%	0.15%	0.44%

In addition to the cost of measurement, the sensitivity of the flowrate measurement is another criterion for evaluating the performance of a flowmeter. The overreading in venturis, which is calculated as the difference of static pressures at the upstream and downstream pressure tappings in Fig. 1, can be used for evaluating the sensitivities of the flowmeters. The overreadings are not affected by the angle of divergent sections and are shown in Fig. 2 for various diameter ratios at a divergent angle of 7°. The overreading for the smallest diameter ratio (0.5) reaches up to 1150 Pa at an air flowrate of around 50 LPM, while up to 506 Pa and 239 Pa overreadings are observed in B6A07 and B7A07 at the same air flowrate. Looking at these figures, one can conclude that the flowmeter with the diameter ratio of 0.5 is most sensitive to air flows. Fig. 2 also shows that the sensitivity of the flowmeters varies with the flowrate, and an average value of sensitivity can be extracted by derivating the pressure drop curves of flowmeters. Sensitivities calculated as arithmetic averages up to 50 LPM of air flowrate were 22.98 Pa/LPM, 10.13 Pa/LPM, and 4.775 Pa/LPM, respectively for B5A07, B6A07, and B7A07 flowmeters. These figures show that a diameter ratio of 0.7 is the least sensitive flowmeter while the highest sensitivity can be obtained with the lowest diameter ratio (0.5). Nonetheless, a diameter ratio of 0.6 (B6A07) can provide enough sensitivity.

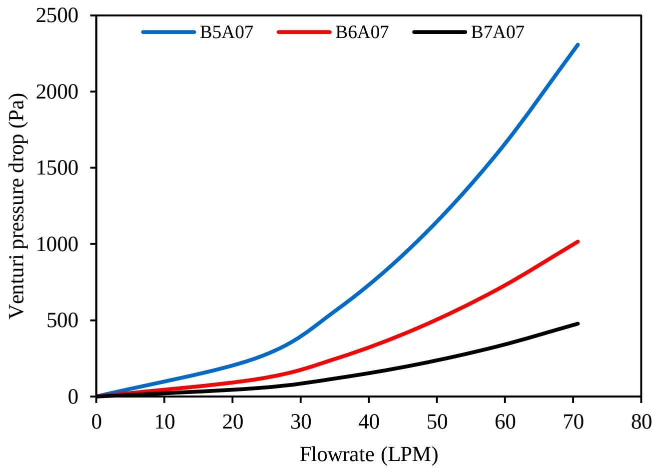

Figure 2. Venturi pressure drops for various flowrates in flowmeters with the lowest costs of measurement

Assuming a normal resolution of a differential pressure sensor of 1 Pa, on the other hand, the change of the overreading signal from 0 to 1 can be used to calculate the minimum detectable air flowrate. Using the data provided in Fig. 2, minimum detectable air flowrates were calculated as 1.83, 2.46, and 3.09 LPM, respectively for B5A07, B6A07, and B7A07 flowmeters. Considering the cost of measurement, the sensitivity, and the minimum detectable air flows, one can conclude that a diameter ratio of 0.6 and a divergent angle of 7° can provide cheaper, yet sensitive enough measurement of flowrate up to 50 LPM.

3.2. Pressure and Flow Fields

Pressure and flow fields for all mini flowmeters were calculated using ANSYS Fluent. Fig. 3 shows pressure fields. For all flowmeters, the static pressures on the inlet side were higher up to around 300 Pa, and the pressure drop over the convergent section was negligible. The highest pressure was observed for the flowmeter with the lowest diameter ratio (0.5) and the highest divergent angle (15°) as 304 Pa. Since the outlet of the flowmeters were set as pressure outlet with gage pressure equal to zero, the highest pressure on the inlet sides of the flowmeters also correspond to the overall pressure drop and cost of flow measurement. Thus, the intensity of red color represents increasing costs. In this aspect, a diameter ratio of 0.5 leads to increased overall pressure drop within the flowmeter, while a diameter ratio of 0.6 offers an optimal solution for air flow measurement.

In the reducing part connecting the convergent section to the throat, the static pressure starts dropping at a high rate, and it reaches its minimum value at the center of the throat. The rate of change of the pressure drop in the throat was the steepest for the lowest diameter ratio of 0.5. The minimum static pressures for a divergent angle of 7° were around -850, -350, and -200 Pa, respectively for diameter ratios of 0.5, 0.6, and 0.7. After the center of the throat, the static pressures starts increasing under the effect of gradually decreasing flow velocity and recovers up to a level below the static pressure at the upstream pressure tappings.

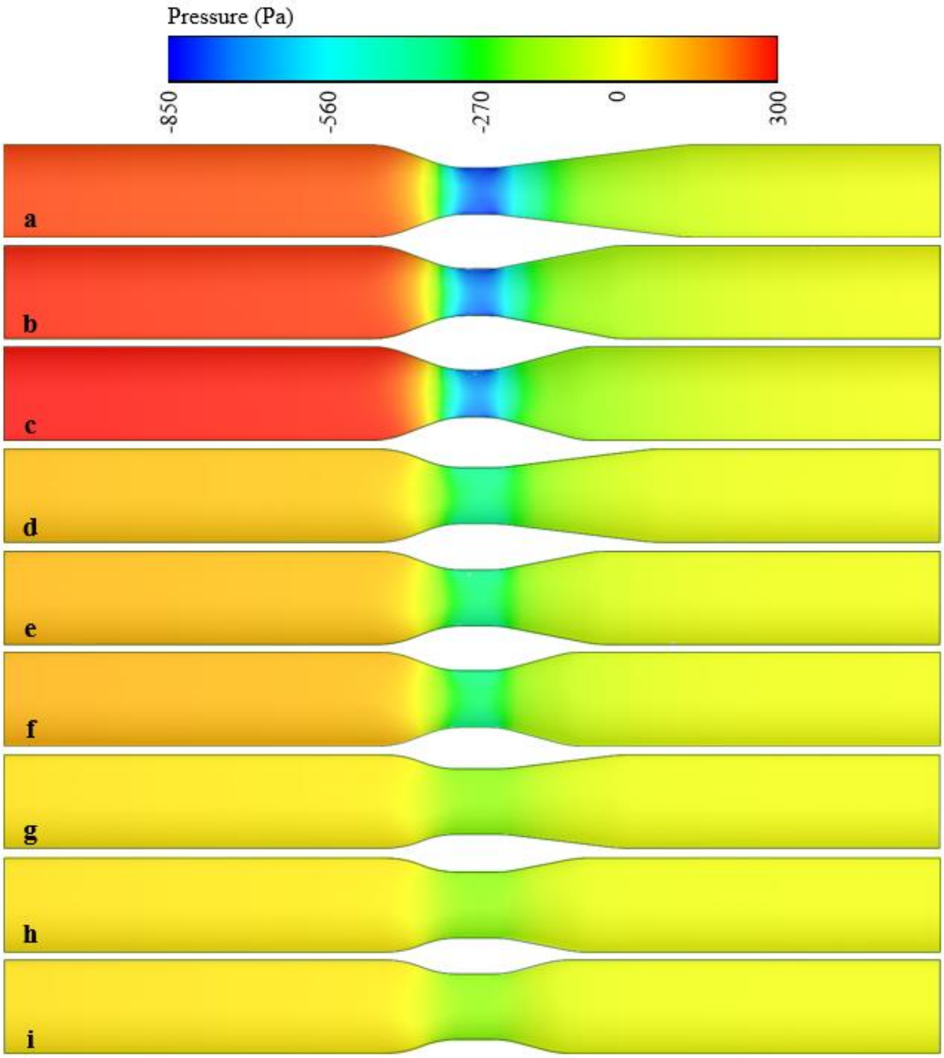

Figure 3. Calculated pressure fields for **a.** B5A07, **b.** B5A11, **c.** B5A15, **d.** B6A07, **e.** B6A11, **f.** B6A15, **g.** B7A07, **h.** B7A11, **i.** B7A15

Calculated velocity vector maps are shown in Fig. 4. The flowmeters with the smallest diameter ratio (Fig. 4.a, 4.b, and 4.c) are the ones with the highest flow velocities within the throat section. The flow velocities reach up to 42 m/s in these flowmeters. The highest flow velocities were around 30 m/s for the diameter ratio of 0.6 (Fig. 4.d, 4.e, and 4.f), and around 20 m/s for the diameter ratio of 0.7 (Fig. 4.g, 4.h, and 4.i). In all flowmeters, starting from the reducing section, the streamlines converged quickly around the center of the throat. This section was the one where negative pressures are observed within the flowmeters (Fig 3). After the throat section, the streamlines recovered. The recovery was the quickest for the diameter ratio of 0.7 and more linear velocity vectors were observed in the divergent section. On the other hand, the recovery was slower for the diameter ratio of 0.5. The distance to the full recovery of streamlines exceeded the enlargement section in all flowmeters with the diameter ratio 0.5. For the diameter ratio of 0.6, the speed of streamline recovery was moderate. For all flowmeters, the streamline recovery was complete before reaching the exit of the venturi meter although it is just complete for the diameter ratio of 0.5. There is evidence that the total length of the venturi flowmeters, which is 100 mm, is long enough to prevent flow distrubances within the device. Thus, the total length of the venturi flowmeters was acceptable for an accurate measurement of the flow.

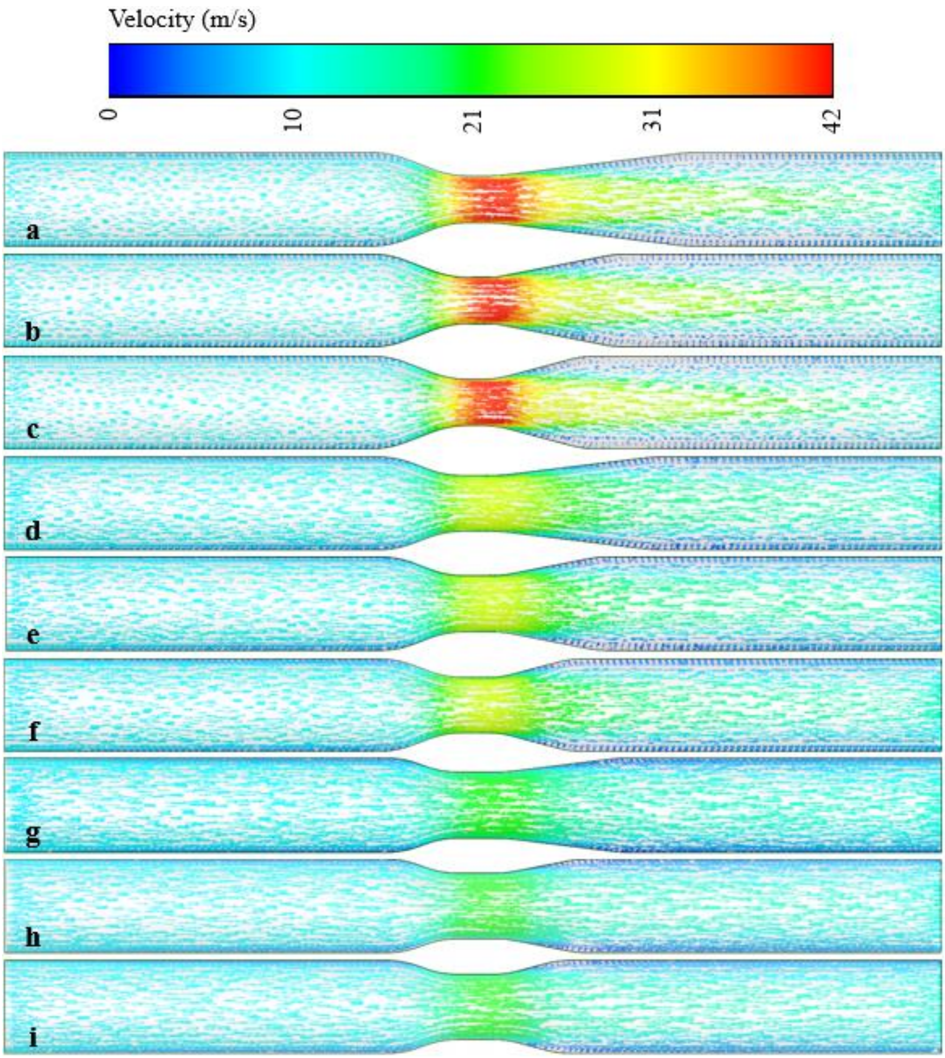

Figure 4. Calculated velocity vectors for **a.** B5A07, **b.** B5A11, **c.** B5A15, **d.** B6A07, **e.** B6A11, **f.** B6A15, **g.** B7A07, **h.** B7A11, **i.** B7A15

4. CONCLUSIONS

Model-based evaluations were performed on mini venturi-type air flowmeters (VTAFs) with various diameter ratios and divergent angles. A total of nine flowmeters with diameter ratios of 0.5, 0.6, and 0.7 and divergent angles of 7°, 11°, and 15° were simulated under steady-state using ANSYS Fluent 2019 R1. Simulations were performed for inlet flow velocities 5, 7.5, 10, 12,5, and 15 m/s of dry air at 20°C. Evaluations were based on the venturi pressure drops, which is the response of the flowmeter to the air flow, and overall pressure drop, which is measured between the inlet and the outlet of the flowmeter and is directly proportional to the cost of air flow measurement. Following conclusions can be withdrawn from the results:

- Although the international standard for venturi flowmeters (ISO 5167-4) does not cover those with pipe sizes less than 50 mm, the results showed that venturi tubes of 10 mm in pipe diameter can be confidently used for measuring air flow in small scale applications.
- Overall pressure drop in a venturi flowmeter is a function of both diameter ratio and divergent angle. Lower divergent angles should be used to reduce overall pressure drop in the venturi flowmeter.
- Venturi flowmeter design must be based on the response of the flowmeter to the air flow, which is the venturi pressure drop. A diameter ratio of 0.6 at 10 mm of pipe diameter can be used to measure air flows up to 50 LPM with satisfactory accuracy and precision.
- With an assumption of the resolution of differential pressure sensor of 1 Pa, a mini venturi-type flowmeter with diameter ratio of 0.6 and pipe size of 10 mm can be used to detect air flows as low as 2.46 LPM at 20°C.

REFERENCES

[1] Kumar P., San S.M., "CFD Study of the Effect of Venturi Convergent and Divergent Angles on Low Pressure Wet Gas Metering", J. Appl. Sci., 14, 3036-3045, 2014.

[2] Zhang F., Dong F., Tan C., "High GVF and low pressure gas-liquid two-phase flow measurement based on dual-cone flowmeter", Flow Meas. Instrum. 21, 410-417, 2010.

[3] Demir S., "A Practical Model for Estimating Pressure Drop in Cyclone Separators: An Experimental Study", Powder Technol. 268, 329-338, 2014.

[4] Demir S., Karadeniz A., Aksel, M., "Effects of cylindrical and conical heights on pressure and velocity fields in cyclones", Powder Technol., 295, 209-217, 2016

[5] Demir S., Karadeniz A., Manav Demir N., Duman S., "Excel VBA-Based Solution to Pipe Flow Measurement Problem", eJSIE, 10(3), 1, 2018.

[6] Huang X., van Sciver S.W., "Performance of a Venturi Flow Meter in Two-Phase Helium Flow", Cryogenics, 36, 303-309, 1996.

[7] Steven R., "Wet Gas Metering with a Horizontally Mounted Venturi Meter", Flow Meas. Instrum., 12, 361-372, 2002.

[8] Lide F., Tao Z., Ningde J., 2007, "A Comparison of Correlations Used for Venturi Wet Gas Metering in Oil and Gas Industry", Journal of Petroleum Science and Engineering, 57, 247-256, 2007.

[9] Steven R., "A Dimensional Analysis of Two Phase Flow Through a Horizontall Installed Venturi Flow Meter", Flow Meas. Instrum., 19, 342-349, 2008.

[10] Steven R., Hall A., "Orifica Plate Meter Wet Gas Flow Performance", Flow Meas. Instrum., 20, 141-151, 2009.

[11] Kumar P., Bing M.W.M., "A CFD Study of Low Pressure Wet Gas Metering Using Slotted Orifice Meters", Flow Meas. Instrum., 22, 33-42, 2011.

[12] He D., Bai B., "A New Correlation for Wet Gas Flow Rate Measurement with Venturi Meter Based on Two-Phase Mass Flow Coefficient", Measurement, 58, 61-67, 2014.

[13] Monni G., de Salve M., Panella B., "Two_phase Flow Measurements at High Void Fraction by a Venturi Meter", Progress in Nuclear Energy 77, 167-175, 2014.
[14] Gajan P., Decaudin Q., Couput J.P., "Analysis of High Pressure Tests on Wet Gas Flow Meterin with a Venturi Meter", Flow Meas. Instrum. 44, 126-131, 2015.
[15] Xu Y., Zhang Q., Zhang T., Ba X., "An Overreading Model for Nonstandard Venturi Meters Based on H Correction Factor", Measurement, 61, 100-106, 2015.
[16] Pan Y., Hong Y., Sun Q., Zheng Z., Wang D., Niu P., "A New Correlation of Wet Gas Flow for Low Pressure with a Vertically Mounted Venturi Meter", Flow Meas. Instrum., 70, 101636, 2019.